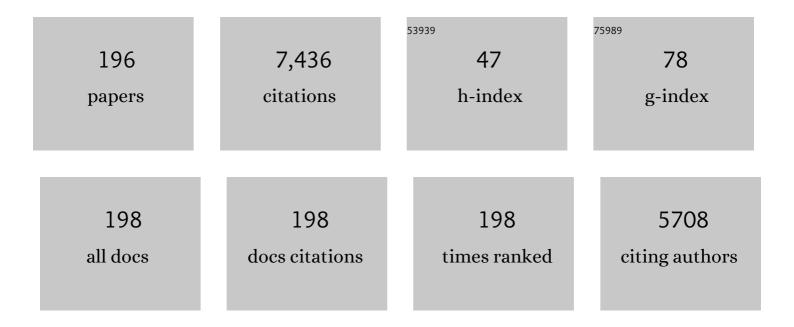
## Michael Moody

List of Publications by Year in descending order

Source: https://exaly.com/author-pdf/6824521/publications.pdf Version: 2024-02-01



#	Article	IF	CITATIONS
1	Atom Probe Tomography of a Cu-Doped TiNiSn Thermoelectric Material: Nanoscale Structure and Optimization of Analysis Conditions. Microscopy and Microanalysis, 2022, 28, 1340-1347.	0.2	3
2	Extending Estimating Hydrogen Content in Atom Probe Tomography Experiments Where H2 Molecule Formation Occurs. Microscopy and Microanalysis, 2022, 28, 1231-1244.	0.2	8
3	Improving the Quantification of Deuterium in Zirconium Alloy Atom Probe Tomography Data Using Existing Analysis Methods. Microscopy and Microanalysis, 2022, 28, 1245-1254.	0.2	2
4	On the influence of microstructure on the neutron irradiation response of HIPed SA508 steel for nuclear applications. Journal of Nuclear Materials, 2022, 559, 153435.	1.3	7
5	Atom Probe Tomography for Isotopic Analysis: Development of the 34S/32S System in Sulfides. Microscopy and Microanalysis, 2022, 28, 1127-1140.	0.2	5
6	Microstructure understanding of high Cr-Ni austenitic steel corrosion in high-temperature steam. Acta Materialia, 2022, 226, 117634.	3.8	32
7	Interaction of transmutation products with precipitates, dislocations and grain boundaries in neutron irradiated W. Materialia, 2022, 22, 101370.	1.3	17
8	Automated calibration of model-driven reconstructions in atom probe tomography. Journal Physics D: Applied Physics, 2022, 55, 375301.	1.3	3
9	Direct observation of hydrogen at defects in multicrystalline silicon. Progress in Photovoltaics: Research and Applications, 2021, 29, 1158-1164.	4.4	9
10	Characterisation of nano-scale precipitates in BOR60 irradiated T91 steel using atom probe tomography. Journal of Nuclear Materials, 2021, 543, 152466.	1.3	6
11	Quantifying the effect of oxygen on micro-mechanical properties of a near-alpha titanium alloy. Journal of Materials Research, 2021, 36, 2529-2544.	1.2	15
12	Characterization of oxidation mechanisms in a family of polycrystalline chromia-forming nickel-base superalloys. Acta Materialia, 2021, 206, 116626.	3.8	17
13	Nanocluster evolution and mechanical properties of ion irradiated T91 ferritic-martensitic steel. Journal of Nuclear Materials, 2021, 548, 152842.	1.3	6
14	Structural and compositional analysis of (InGa)(AsSb)/GaAs/GaP Stranski–Krastanov quantum dots. Light: Science and Applications, 2021, 10, 125.	7.7	14
15	Understanding the Anomalous Short-Range Spatial Correlation Of Fe and Sn in Neutron-Irradiated Zr Alloys. Microscopy and Microanalysis, 2021, 27, 3376-3377.	0.2	0
16	Inter-Experiment Machine Learning on APT experiments: New Insights from Meta-Analysis. Microscopy and Microanalysis, 2021, 27, 182-183.	0.2	0
17	Ex Situ and In Situ Studies of Radiation Damage Mechanisms in Zr-Nb Alloys. , 2021, , 408-434.		2
18	Towards development of a nickel-based oxide dispersion strengthened alloy for use in Molten Salt reactors Microscopy and Microanalysis, 2021, 27, 3378-3378.	0.2	0

#	Article	IF	CITATIONS
19	Atom probe tomography. Nature Reviews Methods Primers, 2021, 1, .	11.8	131
20	The Effect of Analysis Conditions on the Fidelity of Atom Probe Data of Zirconium Alloys. Microscopy and Microanalysis, 2021, 27, 2468-2470.	0.2	0
21	Enhanced Atom Probe Imaging using Generalised Field Evaporation Models. Microscopy and Microanalysis, 2021, 27, 404-406.	0.2	0
22	The role of β-Zr in a Zr-2.5Nb alloy during aqueous corrosion: A multi-technique study. Acta Materialia, 2021, 215, 117042.	3.8	14
23	The Kinetics of Primary Alpha Plate Growth in Titanium Alloys. Metallurgical and Materials Transactions A: Physical Metallurgy and Materials Science, 2020, 51, 131-141.	1.1	14
24	Nanoscale analysis of ion irradiated ODS 14YWT ferritic alloy. Journal of Nuclear Materials, 2020, 528, 151852.	1.3	17
25	The effect of hydrogen on the early stages of oxidation of a magnesium alloy. Corrosion Science, 2020, 165, 108391.	3.0	8
26	Using alpha hulls to automatically and reproducibly detect edge clusters in atom probe tomography datasets. Materials Characterization, 2020, 160, 110078.	1.9	7
27	Electron microscopy and atom probe tomography of nanoindentation deformation in oxide dispersion strengthened steels. Materials Characterization, 2020, 167, 110477.	1.9	4
28	The Effects of Chemistry Variations in New Nickel-Based Superalloys for Industrial Gas Turbine Applications. Metallurgical and Materials Transactions A: Physical Metallurgy and Materials Science, 2020, 51, 4902-4921.	1.1	15
29	Atom probe characterisation of segregation driven Cu and Mn–Ni–Si co-precipitation in neutron irradiated T91 tempered-martensitic steel. Materialia, 2020, 14, 100946.	1.3	5
30	Processing APT Spectral Backgrounds for Improved Quantification. Microscopy and Microanalysis, 2020, 26, 964-977.	0.2	10
31	New insights into the oxidation mechanisms of a Ferritic-Martensitic steel in high-temperature steam. Acta Materialia, 2020, 194, 522-539.	3.8	46
32	Microstructural understanding of the oxidation of an austenitic stainless steel in high-temperature steam through advanced characterization. Acta Materialia, 2020, 194, 321-336.	3.8	58
33	The effect of composition variations on the response of steels subjected to high fluence neutron irradiation. Materialia, 2020, 11, 100717.	1.3	14
34	Reflections on the Analysis of Interfaces and Grain Boundaries by Atom Probe Tomography. Microscopy and Microanalysis, 2020, 26, 247-257.	0.2	30
35	Atom Probe Tomography Study of Gettering in High-Performance Multicrystalline Silicon. IEEE Journal of Photovoltaics, 2020, 10, 863-871.	1.5	9
36	A more holistic characterisation of internal interfaces in a variety of materials via complementary use of transmission Kikuchi diffraction and Atom probe tomography. Applied Surface Science, 2020, 528, 147011.	3.1	7

#	Article	IF	CITATIONS
37	Towards model-driven reconstruction in atom probe tomography. Journal Physics D: Applied Physics, 2020, 53, 475303.	1.3	15
38	The Role of Oxygen in α2 Formation in the Titanium Model Alloy Ti-7Al. MATEC Web of Conferences, 2020, 321, 04003.	0.1	1
39	Combined APT, TEM and SAXS Characterisation of Nanometre-Scale Precipitates in Titanium Alloys. Microscopy and Microanalysis, 2019, 25, 2516-2517.	0.2	1
40	Atom Probe Tomography Analyses of Solute Segregation in Self-Ion Irradiated Electron-Beam Welded SA508 Grade 3 Reactor Pressure Vessel Steels. Microscopy and Microanalysis, 2019, 25, 2520-2521.	0.2	0
41	Fast modelling of field evaporation in atom probe tomography using level set methods. Journal Physics D: Applied Physics, 2019, 52, 435305.	1.3	12
42	A multi-technique study of "barrier layer―nano-porosity in Zr oxides during corrosion and hydrogen pickup using (S)TEM, TKD, APT and NanoSIMS. Corrosion Science, 2019, 158, 108109.	3.0	15
43	Atom Probe Tomography of Au–Cu Bimetallic Nanoparticles Synthesized by Inert Gas Condensation. Journal of Physical Chemistry C, 2019, 123, 26481-26489.	1.5	7
44	Fast Continuum Models for Atom Probe Simulation and Reconstruction. Microscopy and Microanalysis, 2019, 25, 288-289.	0.2	0
45	Observing hydrogen in steel using cryogenic atom probe tomography: A simplified approach. International Journal of Hydrogen Energy, 2019, 44, 32280-32291.	3.8	25
46	Radiation-induced segregation in W-Re: from kinetic Monte Carlo simulations to atom probe tomography experiments. European Physical Journal B, 2019, 92, 1.	0.6	15
47	A Nanoscale Investigation of Carlin-Type Gold Deposits: An Atom-Scale Elemental and Isotopic Perspective. Economic Geology, 2019, 114, 1123-1133.	1.8	47
48	Decoration of voids with rhenium and osmium transmutation products in neutron irradiated single crystal tungsten. Scripta Materialia, 2019, 173, 96-100.	2.6	41
49	Observation of internal oxidation in a 20% cold-worked Fe-17Cr-12Ni stainless steel through high-resolution characterization. Scripta Materialia, 2019, 173, 144-148.	2.6	25
50	Atom Probe Tomography Investigations of Microstructural Evolution in an Aged Nickel Superalloy for Exhaust Applications. Metallurgical and Materials Transactions A: Physical Metallurgy and Materials Science, 2019, 50, 1862-1872.	1.1	12
51	Insight into the impact of atomic- and nano-scale indium distributions on the optical properties of InGaN/GaN quantum well structures grown on m-plane freestanding GaN substrates. Journal of Applied Physics, 2019, 125, 225704.	1.1	5
52	Identification of colloidal silica polishing induced contamination in silicon. Materials Characterization, 2019, 152, 239-244.	1.9	3
53	Atom Probe Tomography of Carbides in Feâ€Crâ€(W)â€C Steels. Steel Research International, 2019, 90, 1900107	7.1.0	1
54	Partitioning of Ti and Kinetic Growth Predictions on the Thermally Grown Chromia Scale of a Polycrystalline Nickel-Based Superalloy. Metallurgical and Materials Transactions A: Physical Metallurgy and Materials Science, 2019, 50, 3024-3029.	1.1	16

#	Article	IF	CITATIONS
55	An in-situ approach for preparing atom probe tomography specimens by xenon plasma-focussed ion beam. Ultramicroscopy, 2019, 202, 121-127.	0.8	29
56	DF-Fit: A Robust Algorithm for Detection of Crystallographic Information in Atom Probe Tomography Data. Microscopy and Microanalysis, 2019, 25, 331-337.	0.2	6
57	A Gas-Phase Reaction Cell for Modern Atom Probe Systems. Microscopy and Microanalysis, 2019, 25, 410-417.	0.2	10
58	Effect of Nb and Fe on damage evolution in a Zr-alloy during proton and neutron irradiation. Acta Materialia, 2019, 165, 603-614.	3.8	44
59	Nanoscale structural and chemical analysis of F-implanted enhancement-mode InAlN/GaN heterostructure field effect transistors. Journal of Applied Physics, 2018, 123, 024902.	1.1	2
60	Impact of local electrostatic field rearrangement on field ionization. Journal Physics D: Applied Physics, 2018, 51, 105601.	1.3	20
61	The effect of oxidation on the subsurface microstructure of a Ti-6Al-4V alloy. Scripta Materialia, 2018, 148, 24-28.	2.6	33
62	Microstructure evolution of T91 irradiated in the BOR60 fast reactor. Journal of Nuclear Materials, 2018, 504, 122-134.	1.3	47
63	A novel ultra-high strength maraging steel with balanced ductility and creep resistance achieved by nanoscale Î <sup>2</sup> -NiAl and Laves phase precipitates. Acta Materialia, 2018, 149, 285-301.	3.8	135
64	Characterization of Phase Chemistry and Partitioning in a Family of High-Strength Nickel-Based Superalloys. Metallurgical and Materials Transactions A: Physical Metallurgy and Materials Science, 2018, 49, 2302-2310.	1.1	22
65	Characterizing solute hydrogen and hydrides in pure and alloyed titanium at the atomic scale. Acta Materialia, 2018, 150, 273-280.	3.8	81
66	Effect of alloying elements on microstructural evolution in oxygen content controlled Ti-29Nb-13Ta-4.6Zr (wt%) alloys for biomedical applications during aging. Materials Science & Engineering A: Structural Materials: Properties, Microstructure and Processing, 2018, 709, 312-321.	2.6	28
67	Correlative atomic scale characterisation of secondary carbides in M50 bearing steel. Philosophical Magazine, 2018, 98, 766-782.	0.7	19
68	Atom probe Tomography of fast-diffusing impurities and the effect of gettering in multicrystalline silicon. AIP Conference Proceedings, 2018, , .	0.3	5
69	Interpreting Atom Probe Data from Oxide–Metal Interfaces. Microscopy and Microanalysis, 2018, 24, 342-349.	0.2	8
70	Microstructural and mechanical characterisation of Fe-14Cr-0.22Hf alloy fabricated by spark plasma sintering. Journal of Alloys and Compounds, 2018, 762, 678-687.	2.8	10
71	Atom probe tomography analysis of the reference zircon gj-1: An interlaboratory study. Chemical Geology, 2018, 495, 27-35.	1.4	27
72	Extending continuum models for atom probe simulation. Materials Characterization, 2018, 146, 299-306.	1.9	9

#	Article	IF	CITATIONS
73	Understanding irradiation-induced nanoprecipitation in zirconium alloys using parallel TEM and APT. Journal of Nuclear Materials, 2018, 510, 460-471.	1.3	17
74	Understanding Corrosion and Hydrogen Pickup of Zirconium Fuel Cladding Alloys: The Role of Oxide Microstructure, Porosity, Suboxides, and Second-Phase Particles. , 2018, , 93-126.		13
75	The atomic structure of polar and non-polar InGaN quantum wells and the green gap problem. Ultramicroscopy, 2017, 176, 93-98.	0.8	24
76	Nanoscale Stoichiometric Analysis of a High-Temperature Superconductor by Atom Probe Tomography. Microscopy and Microanalysis, 2017, 23, 414-424.	0.2	18
77	A nexus between 3D atomistic data hybrids derived from atom probe microscopy and computational materials science: A new analysis of solute clustering in Al-alloys. Scripta Materialia, 2017, 131, 93-97.	2.6	19
78	Atom Probe Analysis of <i>Ex Situ</i> Gas-Charged Stable Hydrides. Microscopy and Microanalysis, 2017, 23, 307-313.	0.2	6
79	Validity of Vegard's rule for Al1â^xInxN (0.08  <  x  <  0.28) thin films gro Physics D: Applied Physics, 2017, 50, 205107.	own on Ga	aN templates 10
80	Detecting Clusters in Atom Probe Data with Gaussian Mixture Models. Microscopy and Microanalysis, 2017, 23, 269-278.	0.2	23
81	Comparing the Consistency of Atom Probe Tomography Measurements of Small-Scale Segregation and Clustering Between the LEAP 3000 and LEAP 5000 Instruments. Microscopy and Microanalysis, 2017, 23, 227-237.	0.2	18
82	On the microtwinning mechanism in a single crystal superalloy. Acta Materialia, 2017, 135, 314-329.	3.8	102
83	Radiation induced segregation and precipitation behavior in self-ion irradiated Ferritic/Martensitic HT9 steel. Journal of Nuclear Materials, 2017, 491, 162-176.	1.3	35
84	On the breakaway oxidation of Fe9Cr1Mo steel in high pressure CO2. Acta Materialia, 2017, 130, 361-374.	3.8	53
85	Automated Atom-By-Atom Three-Dimensional (3D) Reconstruction of Field Ion Microscopy Data. Microscopy and Microanalysis, 2017, 23, 255-268.	0.2	16
86	Direct observation of individual hydrogen atoms at trapping sites in a ferritic steel. Science, 2017, 355, 1196-1199.	6.0	224
87	An Atom Probe Tomography study of site preference and partitioning in a nickel-based superalloy. Acta Materialia, 2017, 125, 156-165.	3.8	113
88	Sequential nucleation of phases in a 17-4PH steel: Microstructural characterisation and mechanical properties. Acta Materialia, 2017, 125, 38-49.	3.8	121
89	High Fidelity Reconstruction of Experimental Field Ion Microscopy Data by Atomic Relaxation Simulations. Microscopy and Microanalysis, 2017, 23, 642-643.	0.2	5
90	A SANS and APT study of precipitate evolution and strengthening in a maraging steel. Materials Science & Engineering A: Structural Materials: Properties, Microstructure and Processing, 2017, 702, 414-424.	2.6	31

#	Article	IF	CITATIONS
91	Specimen preparation methods for elemental characterisation of grain boundaries and isolated dislocations in multicrystalline silicon using atom probe tomography. Materials Characterization, 2017, 131, 472-479.	1.9	11
92	Atomistic Simulations of Surface Effects Under High Electric Fields. Microscopy and Microanalysis, 2017, 23, 644-645.	0.2	1
93	Simplifying Observation of Hydrogen Trapping in Atom Probe Tomography. Microscopy and Microanalysis, 2017, 23, 620-621.	0.2	1
94	Single-Ion Deconvolution of Mass Peak Overlaps for Atom Probe Microscopy. Microscopy and Microanalysis, 2017, 23, 300-306.	0.2	20
95	Ion-irradiation induced clustering in W-Re-Ta, W-Re and W-Ta alloys: An atom probe tomography and nanoindentation study. Acta Materialia, 2017, 124, 71-78.	3.8	107
96	On the composition of microtwins in a single crystal nickel-basedÂsuperalloy. Scripta Materialia, 2017, 127, 37-40.	2.6	59
97	The effect of boron on oxide scale formation in a new polycrystalline superalloy. Scripta Materialia, 2017, 127, 156-159.	2.6	19
98	Application of Atom Probe Tomography to Nitride Semiconductors. Microscopy and Microanalysis, 2017, 23, 666-667.	0.2	0
99	Insights into microstructural interfaces in aerospace alloys characterised by atom probe tomography. Materials Science and Technology, 2016, 32, 232-241.	0.8	20
100	Effect of the milling atmosphere on the microstructure and mechanical properties of a ODS Fe-14Cr model alloy. Materials Science & Engineering A: Structural Materials: Properties, Microstructure and Processing, 2016, 671, 264-274.	2.6	15
101	The microstructure of non-polar a-plane (112Â <sup>-</sup> 0) InGaN quantum wells. Journal of Applied Physics, 2016, 119, .	1.1	22
102	Optimisation of sample preparation and analysis conditions for atom probe tomography characterisation of low concentration surface species. Semiconductor Science and Technology, 2016, 31, 084004.	1.0	6
103	Advances in atom probe tomography instrumentation: Implications for materials research. MRS Bulletin, 2016, 41, 40-45.	1.7	28
104	The formation of ordered clusters in Ti–7Al and Ti–6Al–4V. Acta Materialia, 2016, 112, 141-149.	3.8	44
105	Atomic-scale Studies of Uranium Oxidation and Corrosion by Water Vapour. Scientific Reports, 2016, 6, 25618.	1.6	28
106	Behavior of molecules and molecular ions near a field emitter. New Journal of Physics, 2016, 18, 033031.	1.2	130
107	Continuous and discontinuous precipitation in Fe-1 at.%Cr-1 at.%Mo alloy upon nitriding; crystal structure and composition of ternary nitrides. Philosophical Magazine, 2016, 96, 1509-1537.	0.7	18
108	A mechanistic study of the temperature dependence of the stress corrosion crack growth rate in SUS316 stainless steels exposed to PWR primary water. Acta Materialia, 2016, 114, 15-24.	3.8	50

#	Article	IF	CITATIONS
109	Precipitation of the ordered α 2 phase in a near- α titanium alloy. Scripta Materialia, 2016, 117, 81-85.	2.6	40
110	Secondary precipitation within the cementite phase of reactor pressure vessel steels. Scripta Materialia, 2016, 115, 118-122.	2.6	14
111	On the effect of boron on grain boundary character in a new polycrystalline superalloy. Acta Materialia, 2016, 103, 688-699.	3.8	149
112	Oxidation behaviour of a next generation polycrystalline Mn containing Ni-based superalloy. Scripta Materialia, 2016, 113, 51-54.	2.6	33
113	Practical Issues for Atom Probe Tomography Analysis of III-Nitride Semiconductor Materials. Microscopy and Microanalysis, 2015, 21, 544-556.	0.2	25
114	Structural, electronic, and optical properties of <mml:math xmlns:mml="http://www.w3.org/1998/Math/MathML"&gt;<mml:mi>m</mml:mi>-plane InGaN/GaN quantum wells: Insights from experiment and atomistic theory. Physical Review B, 2015, 92, .</mml:math 	1.1	57
115	In-Situ Deuterium Charging for Direct Detection of Hydrogen in Vanadium by Atom Probe Tomography. Microscopy and Microanalysis, 2015, 21, 695-696.	0.2	7
116	A combined approach for deposition and characterization of atomically engineered catalyst nanoparticles. Journal of Lithic Studies, 2015, 1, 125-131.	0.1	12
117	Atom probe tomography of stress corrosion crack tips in SUS316 stainless steels. Corrosion Science, 2015, 98, 661-671.	3.0	57
118	Thermal–mechanical fatigue behaviour of a new single crystal superalloy: Effects of Si and Re alloying. Acta Materialia, 2015, 95, 456-467.	3.8	38
119	Mining information from atom probe data. Ultramicroscopy, 2015, 159, 324-337.	0.8	50
120	Using transmission Kikuchi diffraction to study intergranular stress corrosion cracking in type 316 stainless steels. Micron, 2015, 75, 1-10.	1.1	39
121	An atom probe tomography study of the oxide–metal interface of an oxide intrusion ahead of a crack in a polycrystalline Ni-based superalloy. Scripta Materialia, 2015, 97, 41-44.	2.6	34
122	Imaging of radiation damage using complementary field ion microscopy and atom probe tomography. Ultramicroscopy, 2015, 159, 387-394.	0.8	18
123	Quantification of oxide particle composition in model oxide dispersion strengthened steel alloys. Ultramicroscopy, 2015, 159, 360-367.	0.8	48
124	Indium clustering in <i>a</i> -plane InGaN quantum wells as evidenced by atom probe tomography. Applied Physics Letters, 2015, 106, .	1.5	46
125	From solid solution to cluster formation of Fe and Cr in $\hat{I}\pm$ -Zr. Journal of Nuclear Materials, 2015, 467, 320-331.	1.3	23
126	Restoring the lattice of Si-based atom probe reconstructions for enhanced information on dopant positioning. Ultramicroscopy, 2015, 159, 314-323.	0.8	19

#	Article	IF	CITATIONS
127	A New Polycrystalline Co-Ni Superalloy. Jom, 2014, 66, 2495-2501.	0.9	59
128	Atomic Imaging of Carbon-Supported Pt, Pt/Co, and Ir@Pt Nanocatalysts by Atom-Probe Tomography. ACS Catalysis, 2014, 4, 695-702.	5.5	50
129	Oxidation and Surface Segregation Behavior of a Pt–Pd–Rh Alloy Catalyst. Journal of Physical Chemistry C, 2014, 118, 26130-26138.	1.5	26
130	Atomically resolved tomography to directly inform simulations for structure–property relationships. Nature Communications, 2014, 5, 5501.	5.8	53
131	Quantitative analysis of carbon in cementite using pulsed laser atom probe. Ultramicroscopy, 2014, 147, 51-60.	0.8	37
132	Low-energy EDX – A novel approach to study stress corrosion cracking in SUS304 stainless steel via scanning electron microscopy. Micron, 2014, 66, 16-22.	1.1	9
133	Resolving the Morphology of Niobium Carbonitride Nano-Precipitates in Steel Using Atom Probe Tomography. Microscopy and Microanalysis, 2014, 20, 1100-1110.	0.2	30
134	The rise of computational techniques in atom probe microscopy. Current Opinion in Solid State and Materials Science, 2013, 17, 224-235.	5.6	25
135	Defining clusters in APT reconstructions of ODS steels. Ultramicroscopy, 2013, 132, 271-278.	0.8	65
136	Solute redistribution in the nanocrystalline structure formed in bearing steels. Scripta Materialia, 2013, 69, 630-633.	2.6	62
137	Spatial decomposition of molecular ions within 3D atom probe reconstructions. Ultramicroscopy, 2013, 132, 92-99.	0.8	5
138	Level Set Methods for Modelling Field Evaporation in Atom Probe. Microscopy and Microanalysis, 2013, 19, 1709-1717.	0.2	23
139	Nearest neighbour diagnostic statistics on the accuracy of APT solute cluster characterisation. Philosophical Magazine, 2013, 93, 975-989.	0.7	15
140	Short-range order in multicomponent materials. Acta Crystallographica Section A: Foundations and Advances, 2012, 68, 547-560.	0.3	47
141	Atom probe crystallography. Materials Today, 2012, 15, 378-386.	8.3	158
142	Atom Probe Microscopy. Springer Series in Materials Science, 2012, , .	0.4	501
143	Magnetism of Co-doped ZnO epitaxially grown on a ZnO substrate. Physical Review B, 2012, 85, .	1.1	54
144	Effect of Sn Addition in Preprecipitation Stage in Al-Cu Alloys: A Correlative Transmission Electron Microscopy and Atom Probe Tomography Study. Metallurgical and Materials Transactions A: Physical Metallurgy and Materials Science, 2012, 43, 2192-2202.	1.1	34

#	Article	IF	CITATIONS
145	Observations of grain boundary impurities in nanocrystalline Al and their influence on microstructural stability and mechanical behaviour. Acta Materialia, 2012, 60, 1038-1047.	3.8	122
146	Atom probe microscopy investigation of Mg site occupancy within δ′ precipitates in an Al–Mg–Li alloy. Scripta Materialia, 2012, 66, 903-906.	2.6	65
147	Atom probe crystallography: Atomic-scale 3-D orientation mapping. Scripta Materialia, 2012, 66, 907-910.	2.6	57
148	Overcoming challenges in the study of nitrided microalloyed steels using atom probe. Ultramicroscopy, 2012, 112, 32-38.	0.8	15
149	Field Ion Microscopy. Springer Series in Materials Science, 2012, , 9-28.	0.4	1
150	From Field Desorption Microscopy to Atom Probe Tomography. Springer Series in Materials Science, 2012, , 29-68.	0.4	3
151	Specimen Preparation. Springer Series in Materials Science, 2012, , 71-110.	0.4	6
152	Experimental Protocols in Atom Probe Tomography. Springer Series in Materials Science, 2012, , 121-155.	0.4	2
153	Tomographic Reconstruction. Springer Series in Materials Science, 2012, , 157-209.	0.4	4
154	Analysis Techniques for Atom Probe Tomography. Springer Series in Materials Science, 2012, , 213-297.	0.4	7
155	Atom Probe Microscopy and Materials Science. Springer Series in Materials Science, 2012, , 299-311.	0.4	2
156	Estimating the physical clusterâ€size distribution within materials using atomâ€probe. Microscopy Research and Technique, 2011, 74, 799-803.	1.2	24
157	Theory of solute clustering in materials for atom probe. Philosophical Magazine, 2011, 91, 2200-2215.	0.7	22
158	Dynamic reconstruction for atom probe tomography. Ultramicroscopy, 2011, 111, 1619-1624.	0.8	72
159	Advances in the reconstruction of atom probe tomography data. Ultramicroscopy, 2011, 111, 448-457.	0.8	209
160	Atom probe crystallography: Characterization of grain boundary orientation relationships in nanocrystalline aluminium. Ultramicroscopy, 2011, 111, 493-499.	0.8	51
161	Crystallographic structural analysis in atom probe microscopy via 3D Hough transformation. Ultramicroscopy, 2011, 111, 458-463.	0.8	59
162	Field evaporation behavior in [0 0 1] FePt thin films. Ultramicroscopy, 2011, 111, 512-517.	0.8	13

#	ARTICLE	IF	CITATIONS
163	in <mml:math display="inline" xmlns:mml="http://www.w3.org/1998/Math/MathML"><mml:mo´ stretchy="false"&gt;(<mml:msub><mml:mi>Ba</mml:mi><mml:mrow><mml:mn>1</mml:mn><mml:mo< td=""><td>₀&gt;â^'₃/mml 2.9</td><td>:mo&gt;<mml: 48</mml: </td></mml:mo<></mml:mrow></mml:msub></mml:mo´ </mml:math>	₀>â^'₃/mml 2.9	:mo> <mml: 48</mml: 
164	Physical Review Letters, 2011, 106, 247002. Influence of the wavelength on the spatial resolution of pulsed-laser atom probe. Journal of Applied Physics, 2011, 110, .	1.1	16
165	Lattice Rectification in Atom Probe Tomography: Toward True Three-Dimensional Atomic Microscopy. Microscopy and Microanalysis, 2011, 17, 226-239.	0.2	58
166	Impact of laser pulsing on the reconstruction in an atom probe tomography. Ultramicroscopy, 2010, 110, 1215-1222.	0.8	51
167	Challenges Associated with the Characterisation of Nanocrystalline Materials Using Atom Probe Tomography. Materials Science Forum, 2010, 654-656, 2366-2369.	0.3	5
168	Influence of surface migration on the spatial resolution of pulsed laser atom probe tomography. Journal of Applied Physics, 2010, 108, .	1.1	81
169	Spatial Resolution in Atom Probe Tomography. Microscopy and Microanalysis, 2010, 16, 99-110.	0.2	153
170	Quantitative description of atomic architecture in solid solutions: A generalized theory for multicomponent short-range order. Physical Review B, 2010, 82, .	1.1	35
171	A three-dimensional Markov field approach for the analysis of atomic clustering in atom probe data. Philosophical Magazine, 2010, 90, 1657-1683.	0.7	56
172	Advances in the calibration of atom probe tomographic reconstruction. Journal of Applied Physics, 2009, 105, .	1.1	214
173	Qualification of the tomographic reconstruction in atom probe by advanced spatial distribution map techniques. Ultramicroscopy, 2009, 109, 815-824.	0.8	129
174	On the understanding of the microscopic origin of the properties of diluted magnetic semiconductors by atom probe tomography. Journal of Magnetism and Magnetic Materials, 2009, 321, 935-943.	1.0	12
175	Origin of the spatial resolution in atom probe microscopy. Applied Physics Letters, 2009, 95, 034103.	1.5	80
176	Applications of Spatial Distribution Maps for Advanced Atom Probe Reconstruction and Data Analysis. Microscopy and Microanalysis, 2009, 15, 246-247.	0.2	12
177	Tomographic Reconstruction in Atom Probe Microscopy: Past, Present.Â.Â. Future?. Microscopy and Microanalysis, 2009, 15, 10-11.	0.2	8
178	Quantitative binomial distribution analyses of nanoscale likeâ€solute atom clustering and segregation in atom probe tomography data. Microscopy Research and Technique, 2008, 71, 542-550.	1.2	198
179	Estimation of the Reconstruction Parameters for Atom Probe Tomography. Microscopy and Microanalysis, 2008, 14, 296-305.	0.2	143
180	Tracking Nanostructural Evolution in Alloys: Large-Scale Analysis of Atom Probe Tomography Data on		4

11

#	Article	IF	CITATIONS
181	Atom Probe Tomography at The University of Sydney. Advances in Materials Research, 2008, , 187-216.	0.2	2
182	Introduction: Special Issue on Atom Probe Tomography. Microscopy and Microanalysis, 2007, 13, 407-407.	0.2	1
183	New Techniques for the Analysis of Fine-Scaled Clustering Phenomena within Atom Probe Tomography (APT) Data. Microscopy and Microanalysis, 2007, 13, 448-463.	0.2	281
184	Contingency table techniques for three dimensional atom probe tomography. Microscopy Research and Technique, 2007, 70, 258-268.	1.2	61
185	Statistical Tools for the Local Electrode Atom Probe. Microscopy and Microanalysis, 2006, 12, 536-537.	0.2	0
186	Techniques for the Analysis of Clusters and Aggregations within Atom Probe Tomography. Microscopy and Microanalysis, 2006, 12, 1732-1733.	0.2	3
187	Numerical study of the accuracy and efficiency of various approaches for Monte Carlo surface hopping calculations. Journal of Chemical Physics, 2005, 122, 094104.	1.2	20
188	Monte Carlo simulation methodology of the ghost interface theory for the planar surface tension. Journal of Chemical Physics, 2004, 120, 1892-1904.	1.2	16
189	Globally uniform semiclassical surface-hopping wave function for nonadiabatic scattering. Journal of Chemical Physics, 2004, 120, 7383-7390.	1.2	12
190	Curvature-Dependent Surface Tension of a Growing Droplet. Physical Review Letters, 2003, 91, 056104.	2.9	65
191	Phase corrected higher-order expression for surface hopping transition amplitudes in nonadiabatic scattering problems. Journal of Chemical Physics, 2003, 119, 11048-11057.	1.2	13
192	Homogeneous nucleation of droplets from a supersaturated vapor phase. Journal of Chemical Physics, 2002, 117, 6705-6714.	1.2	23
193	Nanobubbles: the big picture. Physica A: Statistical Mechanics and Its Applications, 2002, 314, 696-705.	1.2	130
194	Curvature dependent surface tension from a simulation of a cavity in a Lennard-Jones liquid close to coexistence. Journal of Chemical Physics, 2001, 115, 8967-8977.	1.2	70
195	PosgenPy: An Automated and Reproducible Approach to Assessing the Validity of Cluster Search Parameters in Atom Probe Tomography Datasets. Microscopy and Microanalysis, 0, , 1-10.	0.2	0
196	Developing Atom Probe Tomography to Characterize Sr-Loaded Bioactive Glass for Bone Scaffolding. Microscopy and Microanalysis, 0, , 1-11.	0.2	2